

1 Persistent transcriptional programs are associated with remote 2 memory in diverse cells of the medial prefrontal cortex

3

4

5 Michelle B. Chen^{*1}, Xian Jiang^{*2,3}, Stephen R. Quake^{#1,4}, and Thomas C. Südhof^{#2,3}

6

7 ¹Department of Bioengineering, Stanford University, Stanford, CA 94305

8 ²Department of Molecular and Cellular Physiology, Stanford University, Stanford, CA 94305

9 ³Howard Hughes Medical Institute, Stanford University School of Medicine, Stanford, CA 94305

10 ⁴Chan Zuckerberg Biohub, Stanford, 94305, CA

11

12 *Co-first author

13 #Co-corresponding authors: steve@quake-lab.org (S.R.Q), tcs1@stanford.edu (T.C.S)

14

15

16 Abstract

17 It is thought that memory is stored in ‘engrams’, a subset of neurons that undergo
18 learning-induced alterations. The role of gene-expression during learning and short-term
19 memory has been studied extensively, but little is known about remote memory that can persist
20 for a lifetime. Using long-term contextual fear memory as a paradigm, an activity-dependent
21 transgenic model for engram-specific labeling, and single-cell transcriptomics we probed the
22 gene-expression landscape underlying remote memory consolidation and recall in the medial
23 prefrontal cortex. Remarkably, we find sustained activity-specific transcriptional alterations in
24 diverse populations of neurons that persist even weeks after fear-learning and are distinct from
25 those previously identified in learning. Out of a vast plasticity-coding space, we uncover select
26 membrane-fusion genes that could play important roles in maintaining remote memory traces.
27 Unexpectedly, astrocytes and microglia also acquire new persistent gene signatures upon recall
28 of remote memory, suggesting that they actively contribute to memory circuits. Our discovery of
29 novel distinct gene-expression programs involved in long term memory adds an important
30 dimension of activity-dependent cellular states to existing brain taxonomy atlases and sheds
31 light on the elusive mechanisms of remote memory storage.

32

33

34 Memory is the function of the brain by which information is encoded, stored, and
35 retrieved, and is critical for adaptation and survival. Long-term memories do not form
36 immediately after learning, but develop over time through a process of stabilization, known as
37 consolidation¹⁻³. Previous studies have uncovered important roles of a series of molecular and
38 cellular processes in learning and memory, such as CREB-dependent gene expression, cAMP
39 signaling, and synaptic plasticity⁴⁻⁸. The central role of RNA synthesis and subsequent protein
40 translation was first shown in mice, and mechanistically studied in many organisms⁹. Despite
41 these discoveries, the molecular underpinnings of memory consolidation remain elusive. For
42 instance, while gene expression alterations are found in the first 24 h of learning, it is not clear
43 whether these changes are sustained or new ones are acquired in order to consolidate a long-
44 term memory trace that is resistant to disruption on the scale of weeks or years¹⁰⁻¹². Moreover,
45 the dependence of long term memory on the hippocampus is known to degrade over time, with
46 cortical structures being increasingly important¹³. Recently, the development of transgenic tools
47 that allow the identification of small activated neuronal ensembles based on immediate-early-
48 gene (IEG) expression have allowed the dissection of the molecular mechanisms underlying
49 experience-dependent connectivity and plasticity¹⁴⁻¹⁶. Here, we combine a system for activity-
50 dependent genetic labeling (TRAP2) to access engram-specific cells¹⁷⁻¹⁹, an established model
51 of learning and memory (contextual-fear conditioning), and single-cell transcriptomics to
52 uncover the role of gene expression in long term memory storage. We find that cells activated
53 by remote memory recall exhibit sustained transcriptional changes that are both activity-
54 dependent and experience-specific, and that are distinct from the genes expressed during
55 memory encoding. Importantly, we begin to resolve the heterogeneity of plasticity mechanisms
56 via identification of specific genes that have the potential to regulate, enhance, or disrupt long
57 term memory storage.

58

59 ***Molecular characterization of active neuronal populations during remote memory*** 60 ***consolidation***

61 The ability to resolve and characterize an experience-specific neuronal ensemble out of
62 a vast background of neurons is crucial in our understanding of the molecular code that
63 regulates memory formation and storage. The prevailing model for neuronal representation of
64 memory is the Engram Theory²⁰, which posits that learning activates a small ensemble of
65 connected neurons in the brain and induces persistent physical and biochemical changes in the
66 connections between these neurons. These so-called engram cells or “trace cells”, provide

67 physical locations for the storage and retrieval of memories^{21,22}. *TRAP2;Ai14*, a new cFosTRAP
68 transgenic mouse line, is a system that enables the identification of activated neurons via
69 fluorescence by using the immediate-early gene (IEG) *c-Fos* locus to drive the expression of
70 tamoxifen inducible CreER, along with a permanent Cre-dependent tdTomato reporter¹⁹. To
71 identify the transcriptional programs promoting memory consolidation in contextual fear
72 learning, we trained *TRAP2; Ai14* mice in a conditioning chamber with 3 pairs of tone-foot
73 shocks and returned the mice 16 days later for remote contextual memory recall. 4-OHT was
74 injected into the animals immediately prior to memory recall in order to label experience-specific
75 neuronal ensembles. The fear-conditioning followed by recall training paradigm (fear-recall: FR)
76 identifies IEG-expressing neurons during the recall event, the ensemble where memory has
77 been consolidated^{19,23}. In addition, three control groups were implemented: return to context
78 without fear conditioning (no-fear: NF), fear-conditioning without recall (no-recall: NR), and no
79 fear conditioning-nor return (homeage: HC) (**Fig 1a-c**). Together, the collection of TRAPed
80 neurons from each training group allows the comparison of memory consolidation-specific
81 activation versus various forms of baseline activity.

82
83 Samples were collected from the medial prefrontal cortex (mPFC), a cortical region
84 heavily implicated in remote but not short-term memory^{24,25}. To determine whether persisting
85 transcriptional changes exist in the mPFC and to identify such changes, we performed deep
86 plate-based single-cell mRNA sequencing on both TRAP+ and TRAP- cells enriched via flow
87 cytometry, 9 days after the retrieval event (25 days after fear-learning) (**Fig 1d**). This time frame
88 allows adequate time for the *tdT* reporter protein to be expressed¹⁸, and gives access to the
89 persistent transcriptional state of recall-activated cells resulting from remote memory
90 consolidation. The percentage of TRAPed cells collected was significantly higher in FR (~1.5%
91 of all cells) than in other conditions (**Extended Fig 1a**), confirming that the TRAP2 activation
92 captured increased neuronal activity during the fear-recall process. In total, we sequenced 3691
93 neuronal cells (*Snap25+*/tdT+ or tdT-) and 2672 non-neuronal cells from all 4 behavioral
94 trainings, with an average read depth of 1 million reads/cell. An average of ~6000 expressed
95 genes were identified in *Snap25+* neurons (**Extended Fig 1b-c**). Unbiased transcriptome
96 clustering of all cells from all four training conditions allowed the identification of major cell types
97 and confirmed the dominance of neurons in the positive sorting gate, whereas both non-
98 neuronal and neuronal cells (*Cldn5+* endothelial, *Pdgfra+* OPCs, *Cx3cr1+* microglia, *Aqp4+*
99 astrocytes) were present in the negative gate (**Fig 1d-e, Extended Figure 1d**). The enrichment
100 of *tdTomato* mRNA in our putative positive gate was also confirmed. Both TRAP+ and TRAP-

101 cells from FR training groups and three controls (NR, NF, and HC) were represented in all
102 clusters, suggesting that neither the neuronal activation state nor the training paradigm
103 significantly alters cell-type identities on a larger scale (**Fig 1d**).

104
105 Sub-setting and re-clustering all 3691 neurons revealed 7 putative neuron sub-
106 populations - 4 glutamatergic (C0, C2, C3, C5) and 3 GABAergic (C2, C4, C6) - all of which
107 were consistently observed throughout 4 biological replicates (**Fig 2a-c, Extended Fig 2a**).
108 Analysis of enriched genes per neuronal subtype show molecularly distinct populations (**Fig 2d**),
109 with each subtype expressing at least one highly distinctive marker (>90% expression, **Fig 2e**).
110 All subtypes contain *tdT+* cells, indicating the ability of all neuron subtypes to be activated,
111 regardless of the training states (**Extended Fig 2b**). Comparisons of key marker genes (C0-
112 *Dkk11*, C1-*Rprm*, C2-*Calb2*, C3-*Tesc*, C4-*Tnfrsf8l3*, C5-*Tshz*, C6-*Lhx5*) to existing cortical
113 single cell expression databases (Zeisel et al., 2018; Allen Brain Atlas) confirmed their presence
114 in the mPFC as well as their layer specificities (**Extended Fig 2c**).

115
116 To understand whether fear memory consolidation involves the differential activation of
117 distinct neuron subtypes compared to baseline activity, we compared the subtype composition
118 of TRAPed populations collected from FR and NF control mice (**Fig 2f, Extended Fig 2d**).
119 Surprisingly, no significant differences between the FR and NF groups were found in the ratios
120 of the 7 subtypes. This suggests a lack of training-dependent recruitment of neuron types during
121 consolidation compared to basally active populations in a no-fear memory scenario. Excitatory
122 and inhibitory neuron types were both represented in active FR populations, with glutamatergic
123 cells composing ~60-70%. Additionally, within the same FR brains, active and inactive
124 populations had roughly similar neuron subtype compositions, with the exception of C2-*Calb2*
125 and C3-*Tesc*, suggesting only slight shifts in the recruitment or retirement of neuron subtypes
126 due to activity.

127 128 ***Memory consolidation activates long-lasting transcriptional programs that are*** 129 ***heterogeneous across neuron subtypes***

130 To determine whether consolidation-dependent transcriptional changes occur, we looked
131 for differentially expressed genes (DEGs, $\log_2FC > 0.3$ and $FDR < 0.05$) in TRAPed FR vs NF
132 cells (**Fig 3a**). Single cell resolution enables the comparison of neurons within the same
133 subtype, and comparing active populations allows the discovery of transcriptional programs that
134 are related to memory consolidation rather than baseline activity (**Extended Fig 3a**). Of 23,355

135 genes, 1292 were found to be consolidation-dependent, and expression patterns indicated an
136 overall transcriptional activation, with more genes up- than down-regulated. Interestingly, DEGs
137 were largely distinct between subtypes (**Fig 3b**). This subtype-dependent heterogeneity could
138 be indicative of specialized functional roles rather than one mass population working in unison
139 within the memory trace.

140

141 To begin to understand the biological significance of these genes, we applied a set of
142 strict criteria that were selected to identify the most probable candidate effectors. First, each
143 gene had to be differentially expressed in at least $\frac{3}{4}$ of biological replicates, enforcing
144 reproducibility. Subsequent removal of DEGs that are also differentially expressed between the
145 inactive populations in FR vs NF mice allowed the identification of changes specific to active
146 populations (**Extended Fig 4a**). Next, DEGs must be differentially expressed when FR cells are
147 compared to NR and HC controls, ensuring that DEGs are not just a consequence of a fear
148 experience (**Extended Fig 4b**). Lastly, DEGs further passed a permutation test with shuffled
149 labels. These criteria produced a set of 102 “consolidation-specific DEGs” which were
150 biologically robust and remote memory consolidation-specific (see *Methods*) (**Fig 3c**). Several
151 genes encoded for proteins with regulatory roles, including known transcriptional regulators
152 *Slc30a9*, *Hmg20a*, *Hnrmpk*, *Zfp706*, as well as translation regulating factors *Nck2*, *Alpl1*, and
153 *Eif2ak1*. Interestingly, even among the condensed list of consolidation-specific DEGs, we find
154 strong enrichments in processes including the regulation of: vesicle exocytosis (*Vamp2*, *Gdi2*,
155 *Rab15*, *Rab5a*, *Rab24*, *Atp6v0c*, *Syt13*, *Stx1b*, *Nsf*), trans-membrane transport (*Slc25a46*,
156 *Mfsd14a*, *Tmem50a*, *Gpm6a*, *Mfsd14b*, *Abcf3*), dendritic spine density (*Strip1*, *Pls3*, *Gsk3b*),
157 and long-range intracellular protein transport (*Timm29*, *Atad1*, *Pak1*, *Plehb2*, *Sarnp*, *Rtn3*,
158 *Dmtn*, *Sar1a*, *Hid1*) (**Fig 3c, Extended Fig 3b-c**). While these processes are highly linked to
159 synaptic plasticity, we have identified distinct genes out of an expansive plasticity-related coding
160 space that may dictate the specificity in which two neurons communicate during the
161 maintenance of a remote fear-memory trace. Lastly, more than half of consolidation-specific
162 DEG candidates have known associations with neuronal diseases in the Malacards database,
163 suggesting links between the functional role of these genes to various neuronal dysfunctions
164 (Alzheimer Disease, Neuroblastoma, Schizophrenia) and the regulation of long-term memory.

165

166 Single-cell information also allowed us to probe the diversity of transcriptional programs
167 within each subtype. When cells were clustered by the percentile of their expression level for
168 each DEG within the range of all TRAPed cells, distinct populations of “highly activated” and

169 “lowly activated” cells emerged. This suggests that one transcriptional program is concertedly
170 upregulated and perhaps even co-regulated, during memory consolidation (**Fig 3d**). To
171 determine the subtype-specificity of transcriptional programs, individual neurons from each
172 subtype were assigned an “activation state” (see *Methods*). A cell is considered to be “activated”
173 if 50% of the subtype-specific DEGs tested is expressed above the level of the 90th percentile
174 of the distribution in NF controls. Indeed, the fraction of cells activated with the subtype-specific
175 DEGs was generally highest in the corresponding subtype when compared to the activation
176 levels in other subtypes or in the inactive populations (**Fig 3e, Extended Fig 5a**). Together, this
177 could indicate the presence of subtype-specific common regulatory elements.

178
179 To address this possibility, we analyzed our DEGs using Hypergeometric Optimization of
180 Motif Enrichment (HOMER) to search for common regulatory motifs in an unbiased manner. The
181 search was performed anywhere from -400 to +100 bp of the transcription start-site for each
182 DEG (**Extended Fig 5b**). We found 12 putative *de novo* and 2 known motifs enriched within our
183 target gene set ($p > 0.01$). Unexpectedly, dependencies on *CREB*, *NFKb*, *CBP*, *C/EBP*, *AP-1* -
184 canonical transcriptional regulators of neuronal activity, plasticity and short-term memory
185 retrieval (<24h post-learning)²⁷⁻²⁹ - were absent. In particular, the *HIF1b* binding motif was found
186 in >40% of our target DEG sequences, including synaptic transmission and plasticity-related
187 genes *Rab5a*, *Rab24*, *Vamp2*, *Gdi2*, *Gpm6a*, *Strip1*, *Ptp4a1*, *Trim32*, *Mfsd14a*, *Mfsd14b*, and
188 *Slc25a46*. Interestingly, these findings are in line with recent work supporting a potential dual
189 role for *HIF-1* transcription factors during hippocampal-dependent spatial learning and early
190 consolidation under normoxic conditions³⁰.

191
192 ***Consolidation involves a sustained increase in specific presynaptic vesicle fusion and***
193 ***exocytosis genes***

194 To further elucidate the significance of these consolidation-dependent transcriptional
195 programs, we used STRING to look for known and predicted protein-protein interactions. *K-*
196 *means* clustering of the gene nodes revealed a significantly connected network ($p = 1.75e-06$)
197 that was centered around a large cluster of genes encoding for proteins for vesicle-mediated
198 transport, exocytosis and neurotransmitter secretion, all of which were highly connected
199 (confidence=0.4, **Extended Fig 5c**). Remarkably, 20/102 consolidation-specific DEGs fall within
200 these functional categories. These DEGs include syntaxin-1b (*Stx1b*), synaptotagmin-13
201 (*Syt13*), vesicle-associated membrane protein 2 (*Vamp2*), vesicle-fusing ATPase (*Nsf*), and ras-

202 related protein (*Rab5a*), all of which individually are functionally linked to the SNARE-complex
203 and to vesicle exocytosis at the presynaptic terminal (**Fig 4a**). Interestingly, the two most highly
204 and ubiquitously upregulated genes across subtypes were *Serinc-1* and *Serinc-3*, recently
205 discovered to be serine incorporators³¹. Upon delivering serine to the endoplasmic reticulum,
206 phosphatidylcholine and serine are used to synthesize phosphatidylserine (PS), a component of
207 the inner synaptic membrane. Notably, PS phospholipids were first characterized as a binding
208 partner for synaptotagmins upon exposure to Ca²⁺³²⁻³⁵, which suggests that *Serinc-1* and -3
209 may have important roles in enhancing PS levels and facilitating vesicle membrane fusion
210 during memory consolidation. Finally, *in situ* hybridization confirmed the endogenous
211 proportions of neuronal subtypes in TRAPed populations (**Extended Fig 6a-b**), as well as the
212 upregulated expression of key consolidation-specific genes including *Serinc3*, *Syt13*, *Vamp2*,
213 and *Stx1b* within respective neuron subtypes (**Fig 4b-c, Extended Fig 6c**).

214
215 While synaptic plasticity is known to be required for consolidation, the molecular and
216 cellular mechanisms through which plasticity is achieved can vary widely depending on the
217 experience, brain region and neuron type. Although such diversity is expected, technological
218 limitations in accessing memory engrams and the methods to characterize the transcriptomic
219 landscape of single neurons in a high-throughput manner has limited understanding this
220 diversity. Here, we show for the first time that (1) enhanced membrane-fusion and vesicle-
221 exocytosis may be a critical mode of synaptic strengthening during memory consolidation, (2) a
222 specific-set of exocytosis-related genes is found to be involved out of a vast coding-space which
223 could allow highly unique, experience-specific connections to be made, and (3) these particular
224 transcriptional programs are sustained and thus likely required to maintain the memory trace
225 weeks after learning.

226 227 ***Non-neuronal cells exhibit significant transcriptional changes that are distinct from*** 228 ***neurons***

229 Remarkably, we discovered that non-neuronal cells also exhibited sustained
230 transcriptional changes upon memory consolidation (FR compared to NF mice, **Fig 5a-b,**
231 **Extended Fig 7a-b**). These signatures were distinct from neurons, indicating that distinct non-
232 neuronal programs may exert supporting roles in the maintenance of the remote fear-memory
233 trace. Surprisingly, in all cell types more than 95% of these DEGs were upregulated, suggesting
234 an overall transcriptional activation during consolidation. Not only is this response sustained
235 weeks after the initial learning, it is detected even without enrichment of the non-neuronal cells

236 directly associated with the TRAPed engram cells since the TRAP method is neuron-specific.
237 Thus, it is likely that a robust response of non-neuronal cells contributes to memory
238 consolidation.

239
240 We find that the upregulated transcriptional programs are unique to each cell type. Of
241 605 total unique DEGs, only 100 are shared between two cell types or more. Astrocytes and
242 microglia showed the greatest intersection and number of transcriptional changes, with 181 and
243 308 genes perturbed, respectively, in FR mice ($\log_2FC > 1$ and $FDR < 0.01$) (**Fig 5c**). Most of
244 these DEGs represent largely diverging pathways (**Fig 5d**). In particular, upregulated astrocytic
245 genes were enriched in lipid, cholesterol and steroid metabolic functions (*Gja1*, *Hmgcr*, *Dhcr7*,
246 *Insig1*, *Acsl3*, *Idi1*, *Acsbg1*, *10Asah1*, *Hacd3*) as well as glucose transport (*Abcc5*, *Slc39a1*,
247 *Slc6a1*, *Slc27a1*, *Slco1c1*, *Gnb1*, *Ttyh1*), suggesting that enhanced metabolic support from
248 astrocytes could be required during the neuronal consolidation process. This is particularly
249 interesting given that astrocytes have long been known to support the immensely high energy
250 requirements of neurons, and that astrocyte-neuron metabolic coupling is elevated during
251 neuronal activity^{36,37}. Moreover, 95/181 astrocyte DEGs were also reproduced when comparing
252 FR to NR mice, suggesting that a large portion of these effects is specific to the recall-
253 experience itself and not merely a remnant of the fear experience.

254
255 In contrast, DEGs from microglial cells were enriched in innate immunity (*Il6r*, *Stat6*,
256 *Csf3r*, *Il1a*, *Irf5*, *Cd86*, *Tnfrsf1b*, *Ywhaz*, *Litaf*, *Ptgs1*, *Gdi2*, *Rnf13*) and cytoskeletal re-
257 organization / focal adhesion maintenance (*Cdc42*, *Rhoa*, *Rhoh*, *Prkcd*, *Vasp*, *Arf6*, *Vav1*,
258 *Actr2*) pathways, suggesting that upregulation of specific inflammatory molecules and
259 enhancement of cell migration in microglia may be involved in supporting the maintenance of
260 the memory trace. While less is known regarding the immunomodulatory roles of microglia in
261 memory and learning, previous work has shown that low levels of inflammatory cytokines (such
262 as IL-1, IL-6 and TNF-alpha) can regulate neuronal circuit remodeling and long-term
263 potentiation^{38,39}.

264
265 In addition to neuron-neuron coupling, additional communication programs between
266 neurons and non-neuronal cells may be acquired to support the memory trace over long
267 periods. We looked for the expression of receptors or ligands in non-neuronal cells whose
268 known binding partner⁴⁰ is perturbed in TRAPed FR neurons (**Extended Fig 8a-b**). In particular,
269 we focused on genes that were differentially expressed in both the ligand-bound and receptor-

270 bound cell type with fear-memory consolidation (**Extended Fig 8c**). Interestingly, in FR mice,
271 we find the upregulation of neuronal neurogilins-1 and -3 (*Ngln1*, *Ngln3*) and its binding partner
272 neurexin-1 (*Nrxn1*) on astrocytes. A family of CAMs that is a critical component of the bipartite
273 synapse, neuroligin-neurexin complexes are known to act to enhance neuron-glia adhesions
274 and modulate synaptic function^{41–43}. Thus, the concerted upregulation of these binding pairs in
275 FR mice strongly suggests a role of astrocyte-neurexin-neurogulin interactions in the
276 maintenance of synaptic strength during fear memory storage. Altogether, we show for the first
277 time that non-neuronal cells exhibit consolidation-dependent transcriptional perturbations and
278 that microglia and astrocytes may play particularly important roles via a distinct set of genes that
279 support the remote memory trace.

280

281

282 **Discussion**

283 While high-resolution gene-expression atlases of the brain have provided invaluable
284 information regarding cellular taxonomy^{44–46}, characterization of activity- and experience-
285 dependent cell states within these cell types (including non-neuronal cells) is necessary for
286 understanding how experience modulates synaptic plasticity and neuronal circuitry. In particular,
287 the molecular mechanisms underlying the storage of information within neuronal ensembles,
288 and how precisely gene transcription operates in the conversion of short- to long-term
289 memories, is largely unclear. Here, using a combination of activity-dependent labeling of
290 neurons (TRAP2), contextual fear-conditioning, and single cell transcriptomics, we discover the
291 unexpected existence of sustained and coordinated transcriptional programs within activated
292 neuronal ensembles that likely contribute to long-term memory storage in the mPFC.

293

294 Activity-driven transcription is well established and known to shape cortical function and
295 plasticity⁴⁷. A wide range of stimuli including acute sensory experience, metabolic changes,
296 stress, injury and pharmacological intervention evoke new gene expression programs, typically
297 through the action of activity-dependent IEGs (e.g. *c-Fos*, *Arc*, *Jun*, *Egr1*, *Egr2*, *Homer1*) and
298 TFs that regulate them (including *CREB*, *SRF*, *CRE*, *Nf-kB*, *C/EBP*). Induction of these early-
299 response genes (ERGs) can directly alter synaptic transmission^{47–50}. Recently, scRNA-seq of
300 neurons in the visual cortex 1h after light-stimulus confirmed the presence of canonical
301 stimulus-dependent ERGs such as *Nr4a1*, *Nr4a2*, *Fos*, *Fosl2*, *Egr1*, *Junb*, but also found
302 considerable divergences within the ERG programs across different neuronal and non-neuronal

303 cell types⁵¹. Moreover, transcriptional profiles of neurons 4 h post-stimulation were significantly
304 different, resulting in diverse late response gene (LRG) programs that included secreted
305 neuropeptides and synaptic organizers (e.g. *Cbln4*, *Crh*). Intriguingly, the gene expression
306 programs we found upregulated during memory consolidation (~3 weeks post-learning) are
307 largely non-intersecting with these well-established IEGs that are upregulated immediately
308 following salient novel behavioral experience. While canonical IEGs and ERTFs were likely
309 active during the initial fear-learning, they are nearly absent 25 days post-shock (9 days after
310 retrieval). Instead, the sustained transcriptional changes we discovered are likely experience-
311 and region-specific LRG-like programs that are acquired gradually to consolidate a long-term
312 memory trace. Together, this suggests that the activity-dependent transcriptional landscape
313 cannot merely be generalized across experiences, brain regions, nor time.

314
315 In contrast to transcriptional programs immediately induced by acute sensory
316 experience, those involved in more gradual processes like memory storage are much less
317 understood. A cascade of molecular changes is thought to strengthen ‘engram’ synapses in
318 multiple brain regions, including the amygdala, mPFC, and hippocampus. These changes likely
319 depend on gene-expression, as evidenced by the sensitivity of memory consolidation to broad
320 transcriptional inhibitors^{52,53}. Thus, identifying such gene-expression changes provides a
321 gateway to understanding memory storage. A microarray study in the dentate gyrus revealed
322 the dynamic nature of short-term consolidation (0-24 h post- passive avoidance learning), which
323 is characterized by a perturbation of ~500 genes involved in translation/transcription initiation,
324 cell adhesion, neurotransmission and intercellular trafficking⁵⁴. Recently, Rao-Ruiz et al⁵⁵
325 isolated engram-specific hippocampal neurons for single-cell sequencing 24 h after contextual
326 fear conditioning and found an enrichment of activity-regulated genes (e.g. *Arc*, *Npas4*, *Dusp1*,
327 *Atf3*, *Cdkn1a*), many of which were CREB-dependent. However, these studies were restricted
328 to recent memory (retrieval at <24 h after learning), leaving the mechanisms of remote memory
329 unexplored. In fact, new neural pathways are known to be recruited in cortical structures such
330 as the mPFC over time, suggesting a time-dependent evolution of gene programs as one
331 transitions to remote memory. Indeed, we find that the majority of early activity-dependent gene
332 programs perturbed in activated neurons during recent fear memory retrieval⁵⁵, associative fear-
333 learning⁵⁶, post-visual stimulus,⁵¹ or novel environment exposure⁵⁷ are not found within our
334 memory consolidation DEGs (**Extended Figure 9a-c**). In fact, none of plasticity-related vesicle
335 exocytosis genes we identified were found in these data sets, suggesting the uniqueness of
336 these signature to remote memory consolidation.

337

338 Interestingly, TRAPed neurons in mice with fear but no recall (NR) injected with 4-OHT
339 16d after the fear-conditioning also exhibited sustained transcriptional changes at moderate
340 levels (when compared to NF) (**Extended Fig 10**). However, these DEGs are largely non-
341 intersecting with consolidation-specific DEGs, suggesting that (1) the process of recall further
342 induces new transcriptional programs in a different set of neurons and (2) the experience of fear
343 itself can induce long-lasting gene expression programs.

344

345 It is well established that learning and short-term memory (<24 h post-learning) involves
346 CREB-dependent gene networks^{27,28}. A recent study found that a subset of mPFC neurons
347 activated (and labeled) during fear-learning is involved in remote memory expression and
348 CREB-dependent⁵⁸. However, detailed analysis of memory consolidation DEGs and their
349 upstream regulators did not reveal any canonical activity-regulated transcription factors such as
350 CREB, CBP, NF- κ B, AP-1, or C/EBP^{10,29,59–61}. This suggests that the subset of mPFC neurons
351 activated during remote retrieval may differ from those activated during learning, and that they
352 operate under other regulators. While this does not preclude the requirement of CREB in long
353 term memory storage, our data is the first to show that remote memory storage mechanisms
354 could be governed by a different set of transcriptional and regulatory programs than in learning
355 or recent-memory consolidation (<24 h).

356

357 The ability to form and maintain unique synaptic connections that encode a particular
358 memory out of a vast pool of other experiences requires a highly complex coding-space that is
359 likely both molecular and physical in nature. Indeed, the ability of all mPFC neuron types to be
360 activated during consolidation (**Fig 2f**) and the heterogeneity of the activated transcriptional
361 programs (**Fig 3c**) suggests that discrete neuronal populations play differential roles in
362 maintaining the memory trace and thus expand the coding-space. In particular, genes involved
363 in membrane fusion and vesicle exocytosis are strongly upregulated and distributed across
364 subtypes, including *Vamp2*, *Rab5a*, *Nsf*, *Stx1b*, *Syt13*, *Rab15*, *Gdi2*, *Rtn3*, and *Sar1a*, a number
365 of which are known members of the SNARE-complex^{62,63}. While none of these genes have yet
366 to be described in relation to remote-memory, their increased expression here could indicate
367 particular roles in regulating neurotransmitter release throughout memory consolidation. We
368 also uncover a potentially novel role of *Serinc-1* and *-3* in memory storage, which could function
369 to enhance membrane fusion via Ca²⁺-dependent synaptotagmins. Interestingly,
370 phosphatidylserine (PS) supplements have been long been purported to aid in aging-related

371 memory loss, with the basis that aging is correlated to loss of PS in the mammalian brain^{64,65}.
372 The heterogeneity of transcriptional programs between neuron types and the coordination of
373 specific plasticity-related genes points towards the diversity of plasticity mechanisms during
374 memory consolidation. Taken together, our findings provide important insight into the
375 transcriptional basis of memory consolidation and shed light on the therapeutic potential of
376 targeting consolidation-dependent gene-expression programs to address memory loss or
377 enhancement in neuronal disorders.

378

379 **Acknowledgements**

380

381 We thank Drs. Lu Chen, Mu Zhou, and Jie Li for discussion of the experimental design; S. Kolluru
382 and D. Henderson for assistance in library preparation; N. Neff and J. Okamoto for assistance
383 with sequencing; J. Lui for advice on brain dissociation; Drs. L. Denardo, J. Lui and L. Luo for the
384 gifting and help with TRAP2 line; W. Wang, G. Stanley, F. Horns for helpful discussions and
385 computational assistance. S.R.Q. is a Chan Zuckerberg Investigator.

386

387 **Author Contributions**

388

389 XJ and TCS designed animal experiments. MBC and SRQ designed scRNA-seq experiments.
390 XJ performed animal experiments and brain dissection. MBC performed brain dissociation, flow
391 cytometry, single-cell library preparation and sequencing pipelines. XJ performed *in situ*
392 hybridization and imaging. MBC performed all scRNA-seq data and image analysis, with input
393 from XJ, SRQ and TCS. MBC wrote the manuscript with significant contributions from XJ, SRQ,
394 and TCS. TCS and SRQ oversaw the project.

395

396

397

398

399

400

401 **METHODS**

402 ***Mice***

403 All animal experiments were conducted following protocols approved by the
404 Administrative Panel on Laboratory Animal Care at Stanford University. TRAP2; Ai14 mouse
405 line was kindly gifted from Luo lab at Stanford^{21,23}. TRAP2 mice were heterozygous for the
406 Fos2A-iCreER allele, and homozygous for Ai14. Mice were group-housed (maximum 5 mice per
407 cage) on a 12 h light–dark cycle (7 am to 7 pm, light) with food and water freely available. Male
408 mice 42–49 days of age were used for all the experiments. Mice were handled daily for 3 days
409 before their first behavior experiment.

410 ***Genotyping***

411 The following primers: (For) GAG GGA CTA CCT CCT GTA CC, (Rev) TGC CCA GAG
412 TCA TCC TTG GC were used for genotyping of the Fos2A-iCreER allele.

413 ***Fear conditioning***

414 The fear conditioning training was performed as previously described⁶⁶. Briefly, mice
415 were individually placed in the fear conditioning chamber (Coulbourn Instruments) located in the
416 center of a sound attenuating cubicle, which was cleaned with 10% ethanol to provide a
417 background odor. A ventilation fan provided a background noise at ~55 dB. After a 2 min
418 exploration period, three tone-footshock pairings separated by 1 min intervals were provided.
419 The 85 dB 2 kHz tone lasted for 30 s, and the footshocks were 0.75 mA and lasted for 2 s. The
420 foot shocks co-terminated with the tone. The mice remained in the training chamber for another
421 60 s before being returned to the home cages. For the context recall, mice were placed back
422 into the original conditioning chamber for 5 min 16 days after the training. The behavior of the
423 mice was recorded with the FreezeFrame software and analyzed with the FreezeView software
424 (Coulbourn Instruments). Motionless bouts lasting more than 1 s were considered as freeze.
425 Data were analyzed with the tracking software Viewer III (Biobserve).

426 ***TdTomato florescence examination***

427 Mice were deep anesthetized with tribromoethanol and perfused with PBS followed by
428 fixative (4% paraformaldehyde diluted in PBS). The brains were then removed and postfixated in
429 4 °C overnight and immersed in 30% sucrose solution for 2 days before being sectioned at

430 50 μ m thicknesses on a cryostat (CM3050 S; Leica Biosystems). Imaging was performed with a
431 scanning microscope (BX61VS; OLYMPUS CORPORATION).

432 ***Single-cell dissociation and flow cytometry***

433 mPFC regions were micro-dissected from live vibratome sections (300 μ m thick) of the
434 prefrontal cortex. Tissue pieces were enzymatically dissociated via a papain-based digestion
435 system (Worthington, Cat # LK003150). Briefly, tissue chunks were incubated in 1mL of papain
436 (containing L-cysteine and EDTA), DNase, and kynurenic acid for 1 hour at 37C and 5% CO₂.
437 After 10 min of incubation, tissues were triturated briefly with a P1000 wide bore pipette tip and
438 returned. Cells were triturated another 4 times (~30 each) with a P200 pipette tip over the rest of
439 the remaining incubation time. At room temperature, cell suspensions were centrifuged at 350g
440 for 10 min, resuspended in 1mL of EBSS with 10% v/v ovomucoid inhibitor, 4.5% v/v DNase
441 and 0.1% v/v kynurenic acid, and centrifuged again. Supernatant was removed and cells 1mL
442 ACSF was added. ACSF was composed of: 1mM KCl, 7mM MgCl₂, 0.5 mM CaCl₂, 1.3 mM
443 NaH₂PO₄, 110 mM choline chloride, 24mM NaHCO₃, 1.3 mM Na Ascorbate, 20mM glucose
444 and 0.6mM sodium pyruvate. Cells were passed through a 70 μ m cell strainer to remove debris.
445 Hoescht stain was added (1:2000, Life Technologies, Cat #H3570) and incubated in the dark at
446 4C for 10 min. Samples were centrifuged (350g for 8 min at 4C) and resuspended in 0.5mL of
447 ACSF and kept on ice for flow cytometry.

448 Cells were sorted via the Sony SH800 into 96 or 384 well plates (Biorad) directly into
449 lysis buffer⁶⁷ with oligodT, and immediately snap frozen until processing. A positive “TRAP” gate
450 was set for cells that were both Hoescht+ and tdT+. A negative “TRAP” gate was set for all
451 Hoescht+ and tdT- cells in general. No gating on forward or backscatter was used to avoid size
452 biases that might be present in a heterogenous neuronal population. Each plate was kept on the
453 sorter for <25 min to prevent evaporation.

454 ***Sequencing***

455 Cell lysis, first-strand synthesis and cDNA synthesis was performed using the Smart-seq-
456 2 protocol as described previously⁶⁷ in both 96-well and 384-well formats, with some
457 modifications. After cDNA amplification (23 cycles), cDNA concentrations were determined via
458 capillary electrophoresis (96-well format) or the PicoGreen quantitation assay (384-well format)
459 and wells were cherry-picked to improve quality and cost of sequencing. Cell selection was done
460 through custom scripts and simultaneously normalizes cDNA concentrations to ~0.2 ng/uL per

461 sample, using the TPPLabtech Mosquito HTS and Mantis (Formulatrix) robotic platforms.
462 Libraries were prepared, pooled and cleaned using the Illumina Nextera XT kits or in-house Tn5,
463 following the manufacturer's instructions. Libraries were then sequenced on the Nextseq or
464 Novaseq (Illumina) using 2 x 75bp paired-end reads and 2 x 8bp index reads with a 200 cycle kit
465 (Illumina, 20012861). Samples were sequenced at an average of 1.5M reads per cell.

466

467 **RNA scope**

468 RNAscope experiment was performed following the manufactory's instructions using RNAscope
469 multiplex fluorescent reagent kit v2 (ACD Cat #323100). All probes were purchased from
470 existing stocks of custom designed from ACD.

471 **Bioinformatics and data analysis**

472 *Mapping to the genome*

473 Sequences from the Nextseq or Novaseq were demultiplexed using bcl2fastq, and reads
474 were aligned to the mm10 genome augmented with ERCC sequences, using STAR version
475 2.5.2b. Gene counts were made using HTSEQ version 0.6.1p1. All packages were called and run
476 through a custom Snakemake pipeline. We applied standard algorithms for cell filtration, feature
477 selection, and dimensionality reduction. Briefly, genes appearing in fewer than 5 cells, samples
478 with fewer than 100 genes, and samples with less than 50,000 reads were excluded from the
479 analysis. Out of these cells, those with more than 30% of reads as ERCC, and more than 10%
480 mitochondrial or 10% ribosomal were also excluded from analysis. Counts were log-normalized
481 then scaled where appropriate.

482 Next, the *Canonical Correlation Analysis* function from the Seurat package⁶⁸ was used to
483 align raw data from multiple experiments. Only the first 10 Canonical Components (CCs) were
484 used. After alignment, relevant features were selected by filtering expressed genes to a set of
485 ~2500 with the highest positive and negative pairwise correlations. Genes were then projected
486 into principal component space using the robust principal component analysis (rPCA). Single cell
487 PC scores and genes loadings for the first 20 PCs were used as inputs into Seurat's (v2)
488 *FindClusters* and *RunTsne* functions to calculate 2-dimensional tSNE coordinates and search for
489 distinct cell populations. Briefly, a shared-nearest-neighbor graph was constructed based on the
490 Euclidean distance metric in PC space, and cells were clustered using the Louvain method. Cells
491 and clusters were then visualized using 3-D t-distributed Stochastic Neighbor embedding on the

492 same distance metric. A neuron is characterized as “TRAPed” trapped if it satisfies 2 conditions:
493 (1) from the tdT+ sort gate (tdT protein positive) (2) tdT mRNA raw count > 0. Differential gene
494 expression analysis was done by applying the Mann-Whitney U-test on various cell population.
495 Raw p-values were adjusted via the false discovery rate (FDR). Permutation tests were then
496 performed on all genes of interest. All graphs and analyses were generated and performed in R.
497 GeneAnalytics and GeneCards- packages offered by Gene Set Enrichment Analysis (GSEA) tool
498 was used for GO/KEGG/REACTOME pathway analysis and classification of enriched genes in
499 each subpopulation.

500

501 *Finding “consolidation-specific DEGs”*

502 To reduce our list of DEGs (FR TRAP vs NF TRAP results in 1291 DEGs, cells from 4
503 biological replicates pooled, logFC>0.3, FDR<0.05) to only the most recall-specific, 4 steps
504 were taken. First, DEGs are re-calculated by assessing each experiment individually using the
505 whole transcriptome, and only DEGs that intersect in $\frac{3}{4}$ replicates are kept. While this
506 decreases the statistical power, it ensures biological reproducibility. The 3 out of 4 criteria was
507 chosen as a compromise due to the high strictness of 4 out of 4 which yielded only 7 DEGs. All
508 resulting DEGs are found in the initial DEG list (all replicates pooled). Second, “inactive” (tdT
509 negative) populations were also compared (FR inactive vs NF inactive) and any DEGs which
510 were intersecting with the DEGs left after the first criteria, were removed. This ensures that
511 DEGs are activity-dependent, and not merely an overall upregulation in all cells due to the
512 experience. This routinely removed genes such as *Hsp90aa1* and *Pcna-ps2*. Third, the
513 remaining DEGs had to be differentially expressed when FR TRAP was compared to either FR
514 TRAP and HC TRAP. This ensures that the DEGs are specific to only neuronal ensembles that
515 labeled by memory recall, and not due to forms of baseline activity (HC) or activity remaining
516 from the initial fear learning (NR). Last, the remaining DEGs must pass a permutation test
517 where the training labels are shuffled and a distribution of log2FC is computed based on these
518 labels. The true observed logFC must be above the 95th percentile of the distribution of the
519 shuffled distribution. After placing these constraints, 102 genes remain from the original list of
520 1291.

521 *Assessment of “Activation Score”*

522 A TRAPed (or inactive) cell is considered to be “activated” by the consolidation-DEG
523 program if 25, 50 or 75% of the subtype-specific DEGs (“consolidation-specific DEGs” only) is

524 expressed above the 90th percentile of the distribution of that gene in NF TRAP controls from
525 the same subtype. This calculation is then repeated with DEG programs specific to each
526 neuronal subtype. The fraction of cells activated with the subtype-specific signature is calculated
527 as the number of “activated” cells divided by all cells in the subtype/activity group.

528 *Regulatory Motif analysis*

529 Known and de novo motifs enrichment was found using HOMER by inputting the list of
530 102 consolidation-specific DEGs and using the function *findMotifs.pl* and the criteria ‘*-start -400*
531 *-end 100 -len 8,10 -p 2*’. Motif locations in specific DEGs were found using the *-find <motif file>*
532 option of *findMotifs.pl*.

533 *RNAscope image analysis*

534 Images were taken at using a Nikon Confocal Microscope (at 10X or 20X, NA=0.45) and
535 images were processed in ImageJ to only obtain the mPFC regions. The resulting images were
536 fed into a custom image analysis pipeline was developed on CellProfiler (using a combination of
537 the functions *IdentifyPrimaryObjects*, *RelateObjects*, *FilterObjects*, *MeasureObjectIntensity*,
538 *ClassifyObjects*, and *CalculateMath*. Custom pipeline in SI Methods). Briefly, images were
539 corrected with control slides (unstained sample and negative control probes) and cells were
540 segmented using the DAPI signal. Those harboring a signal (above a set threshold level) for
541 both the subtype marker and tdT probe were retained. The integrated fluorescence intensity of
542 the DEG probe was calculated for each DAPI+/Subtype+/tdT+ cell. Cells that were not double-
543 positive were not considered. The integrated fluorescent intensity was then normalized to the
544 integrated DAPI signal per cell and results were plotted with custom scripts in R.

545

546

547

548

549

550

551 **References**

- 552 1. Lechner, H. A., Squire, L. R., Byrne, J. H. & Mu, G. Remembering Müller and Pilzecker.
553 77–88
- 554 2. Müller, G. E. & Pilzecker, A. *Experimentelle beiträge zur lehre vom gedächtniss.* (J.A.
555 Barth, 1900).
- 556 3. Squire, L. R. Mechanisms of memory. *Science (80-.)*. **232**, 1612 LP – 1619 (1986).
- 557 4. Hebb, D. Organization of Behavior: A Neuropsychological Theory. *John Wiley Sons Inc,*
558 *NJ* (1941). doi:10.1177/000271625027100159
- 559 5. Agranoff, B. W., Davis, R. E., Casola, L. & Lim, R. Actinomycin D Blocks Formation of
560 Memory of Shock-Avoidance in Goldfish. *Science (80-.)*. **158**, 1600 LP – 1601 (1967).
- 561 6. Flexner, J. B., Flexner, L. B. & Stellar, E. Memory in Mice as Affected by Intracerebral
562 Puromycin. *Science (80-.)*. **141**, 57 LP – 59 (1963).
- 563 7. Taubenfeld, S. M., Milekic, M. H., Monti, B. & Alberini, C. M. The consolidation of new but
564 not reactivated memory requires hippocampal C/EBP β . *Nat. Neurosci.* **4**, 813–818
565 (2001).
- 566 8. Kandel, E. R. The Molecular Biology of Memory Storage : A Dialogue Between Genes
567 and Synapses. **294**, 1030–1039 (2015).
- 568 9. Flexner, L. B. & Flexner, J. B. Effect of acetoxycycloheximide and of an
569 acetoxycycloheximide-puromycin mixture on cerebral protein synthesis and memory in
570 mice. **55**, 369–374 (1966).
- 571 10. Alberini, C. M. Transcription factors in long-term memory and synaptic plasticity. *Physiol.*
572 *Rev.* **89**, 121–145 (2009).
- 573 11. Alberini, C. M. & Kandel, E. R. The Regulation of Transcription in Memory Consolidation.
574 *Cold Spring Harb. Perspect. Biol.* **7**, (2015).
- 575 12. Donahue, C. P. *et al.* Transcriptional profiling reveals regulated genes in the
576 hippocampus during memory formation. *Hippocampus* **12**, 821–833 (2002).

- 577 13. Tonegawa, S., Morrissey, M. D. & Kitamura, T. The role of engram cells in the systems
578 consolidation of memory. *Nat. Rev. Neurosci.* **19**, 485–498 (2018).
- 579 14. Reijmers, L. G., Perkins, B. L., Matsuo, N. & Mayford, M. Localization of a Stable Neural
580 Correlate of Associative Memory. *Science (80-.)*. **317**, 1230 LP – 1233 (2007).
- 581 15. Tonegawa, S., Liu, X., Ramirez, S. & Redondo, R. Memory Engram Cells Have Come of
582 Age. *Neuron* **87**, 918–931 (2015).
- 583 16. DeNardo, L. & Luo, L. Genetic strategies to access activated neurons. *Curr. Opin.*
584 *Neurobiol.* **45**, 121–129 (2017).
- 585 17. Allen, W. E. *et al.* Thirst-associated preoptic neurons encode an aversive motivational
586 drive. *Science (80-.)*. **357**, 1149 LP – 1155 (2017).
- 587 18. Guenther, C. J., Miyamichi, K., Yang, H. H., Heller, H. C. & Luo, L. Permanent genetic
588 access to transiently active neurons via TRAP: targeted recombination in active
589 populations. *Neuron* **78**, 773–784 (2013).
- 590 19. DeNardo, L. A. *et al.* Temporal evolution of cortical ensembles promoting remote memory
591 retrieval. *Nat. Neurosci.* **22**, 460–469 (2019).
- 592 20. Semon, R. W. *Die Mneme als erhaltendes Prinzip im Wechsel des organischen*
593 *Geschehens.* . (Engelmann, 1911).
- 594 21. Thompson, R. F. In Search of Memory Traces. *Annu. Rev. Psychol.* **56**, 1–23 (2004).
- 595 22. Josselyn, S. A., Köhler, S. & Frankland, P. W. Finding the engram. *Nat. Rev. Neurosci.*
596 **16**, 521 (2015).
- 597 23. Minatohara, K., Akiyoshi, M. & Okuno, H. Role of Immediate-Early Genes in Synaptic
598 Plasticity and Neuronal Ensembles Underlying the Memory Trace. *Front. Mol. Neurosci.*
599 **8**, 78 (2016).
- 600 24. Euston, D. R., Gruber, A. J. & McNaughton, B. L. The role of medial prefrontal cortex in
601 memory and decision making. *Neuron* **76**, 1057–1070 (2012).
- 602 25. Bontempi, B., Laurent-Demir, C., Destrade, C. & Jaffard, R. Time-dependent

- 603 reorganization of brain circuitry underlying long-term memory storage. *Nature* **400**, 671–
604 675 (1999).
- 605 26. Zeisel, A. *et al.* Molecular Architecture of the Mouse Nervous System. *Cell* **174**, 999–
606 1014.e22 (2018).
- 607 27. Suzuki, A. *et al.* Upregulation of CREB-Mediated Transcription Enhances Both Short- and
608 Long-Term Memory. *J. Neurosci.* **31**, 8786 LP – 8802 (2011).
- 609 28. Kida, S. *et al.* CREB required for the stability of new and reactivated fear memories. *Nat.*
610 *Neurosci.* **5**, 348–355 (2002).
- 611 29. Gass, P. *et al.* Deficits in memory tasks of mice with CREB mutations depend on gene
612 dosage. *Learn. Mem.* **5**, 274–288 (1998).
- 613 30. C O’Sullivan, N., Sheridan, G. & Murphy, K. Transcriptional Profiling of Hippocampal
614 Memory-Associated Synaptic Plasticity: Old Friends and New Faces. in *Transcription*
615 *Factors CREB and NF- κ B: Involvement in Synaptic Plasticity and Memory Formation* 43–
616 65 (Bentham Science Publishers, 2012). doi:10.2174/978160805257811201010043
- 617 31. Inuzuka, M., Hayakawa, M. & Ingi, T. Serinc, an Activity-regulated Protein Family,
618 Incorporates Serine into Membrane Lipid Synthesis. *J. Biol. Chem.* **280**, 35776–35783
619 (2005).
- 620 32. Perin, M. S., Friedt, V. A., Mignery, G. A., Jahn, R. & Li, T. C. S. Phospholipid binding by a
621 synaptic vesicle protein homologous to the regulatory region of protein kinase C. **345**,
622 260–263 (1990).
- 623 33. Brose, N., Petrenko, A. G., Südhof, T. C. & Jahn, R. Synaptotagmin : A Calcium Sensor
624 on the Synaptic Vesicle Surface. **256**, 1021–1026 (1992).
- 625 34. Zhang, X., Rizo, J. & Südhof, T. C. Mechanism of Phospholipid Binding by the C2A-
626 Domain of Synaptotagmin I. *Biochemistry* **37**, 12395–12403 (1998).
- 627 35. Davis, A. F. *et al.* Kinetics of Synaptotagmin Responses to Ca^{2+} and Assembly with the
628 Core SNARE Complex onto Membranes. *Neuron* **24**, 363–376 (1999).
- 629 36. Pellerin, L. & Magistretti, P. J. Glutamate uptake into astrocytes stimulates aerobic

- 630 glycolysis: a mechanism coupling neuronal activity to glucose utilization. *Proc. Natl. Acad.*
631 *Sci. U. S. A.* **91**, 10625–10629 (1994).
- 632 37. Bélanger, M., Allaman, I. & Magistretti, P. J. Brain Energy Metabolism: Focus on
633 Astrocyte-Neuron Metabolic Cooperation. *Cell Metab.* **14**, 724–738 (2011).
- 634 38. Williamson, L. L., Sholar, P. W., Mistry, R. S., Smith, S. H. & Bilbo, S. D. Microglia and
635 Memory: Modulation by Early-Life Infection. *J. Neurosci.* **31**, 15511 LP – 15521 (2011).
- 636 39. Yirmiya, R. & Goshen, I. Immune modulation of learning, memory, neural plasticity and
637 neurogenesis. *Brain. Behav. Immun.* **25**, 181–213 (2011).
- 638 40. Ramilowski, J. A. *et al.* A draft network of ligand–receptor-mediated multicellular
639 signalling in human. *Nat. Commun.* **6**, 7866 (2015).
- 640 41. Knight, D., Xie, W. & Boulianne, G. L. Neurexins and Neuroligins: Recent Insights from
641 Invertebrates. *Mol. Neurobiol.* **44**, 426–440 (2011).
- 642 42. Hillen, A. E. J., Burbach, J. P. H. & Hol, E. M. Cell adhesion and matricellular support by
643 astrocytes of the tripartite synapse. *Prog. Neurobiol.* **165–167**, 66–86 (2018).
- 644 43. Südhof, T. C. Synaptic Neurexin Complexes: A Molecular Code for the Logic of Neural
645 Circuits. *Cell* **171**, 745–769 (2017).
- 646 44. Zeisel, A. *et al.* Cell types in the mouse cortex and hippocampus revealed by single-cell
647 RNA-seq. *Science (80-.)*. **347**, 1138 LP – 1142 (2015).
- 648 45. Saunders, A. *et al.* Molecular Diversity and Specializations among the Cells of the Adult
649 Mouse Brain. *Cell* **174**, 1015-1030.e16 (2018).
- 650 46. Rosenberg, A. B. *et al.* Single-cell profiling of the developing mouse brain and spinal cord
651 with split-pool barcoding. *Science (80-.)*. **360**, 176 LP – 182 (2018).
- 652 47. West, A. E. & Greenberg, M. E. Neuronal Activity–Regulated Gene Transcription in
653 Synapse Development and Cognitive Function. *Cold Spring Harb. Perspect. Biol.* (2011).
- 654 48. Shepherd, J. D. & Bear, M. F. New views of Arc, a master regulator of synaptic plasticity.
655 *Nat. Neurosci.* **14**, 279 (2011).

- 656 49. Sheng, M. & Greenberg, M. E. The regulation and function of c-fos and other immediate
657 early genes in the nervous system. *Neuron* **4**, 477–485 (1990).
- 658 50. Chang, M. C. *et al.* Narp regulates homeostatic scaling of excitatory synapses on
659 parvalbumin-expressing interneurons. *Nat. Neurosci.* **13**, 1090 (2010).
- 660 51. Hrvatin, S. *et al.* Single-cell analysis of experience-dependent transcriptomic states in the
661 mouse visual cortex. *Nat. Neurosci.* **21**, 120–129 (2018).
- 662 52. Chen, D. Y. *et al.* A critical role for IGF-II in memory consolidation and enhancement.
663 *Nature* **469**, 491-U63 (2011).
- 664 53. Igaz, L. M., Vianna, M. R. M., Medina, J. H. & Izquierdo, I. Two Time Periods of
665 Hippocampal mRNA Synthesis Are Required for Memory Consolidation of Fear-Motivated
666 Learning. *J. Neurosci.* **22**, 6781 LP – 6789 (2002).
- 667 54. O’Sullivan, N. C. *et al.* Temporal change in gene expression in the rat dentate gyrus
668 following passive avoidance learning. *J. Neurochem.* **101**, 1085–1098 (2007).
- 669 55. Rao-Ruiz, P. *et al.* Engram-specific transcriptome profiling of contextual memory
670 consolidation. *Nat. Commun.* **10**, 1–14 (2019).
- 671 56. Cho, J.-H., Huang, B. S. & Gray, J. M. RNA sequencing from neural ensembles activated
672 during fear conditioning in the mouse temporal association cortex. *Sci. Rep.* **6**, 31753
673 (2016).
- 674 57. Lacar, B. *et al.* Nuclear RNA-seq of single neurons reveals molecular signatures of
675 activation. *Nat. Commun.* **7**, 11022 (2016).
- 676 58. Matos, M. R. *et al.* Memory strength gates the involvement of a CREB-dependent cortical
677 fear engram in remote memory. *Nat. Commun.* **10**, 1–11 (2019).
- 678 59. Ahn, H. J. *et al.* c-Rel, an NF- κ B family transcription factor, is required for hippocampal
679 long-term synaptic plasticity and memory formation. *Learn. Mem.* **15**, 539–549 (2008).
- 680 60. Bourtchuladze, R. *et al.* Deficient long-term memory in mice with a targeted mutation of
681 the cAMP-responsive element-binding protein. *Cell* **79**, 59–68 (1994).

- 682 61. Sakamoto, K., Karelina, K. & Obrietan, K. CREB: a multifaceted regulator of neuronal
683 plasticity and protection. *J. Neurochem.* **116**, 1–9 (2011).
- 684 62. Ungermann, C. & Langosch, D. Functions of SNAREs in intracellular membrane fusion
685 and lipid bilayer mixing. *J. Cell Sci.* **118**, 3819 LP – 3828 (2005).
- 686 63. Südhof, T. C. & Rothman, J. E. Membrane Fusion: Grappling with SNARE and SM
687 Proteins. *Science (80-.)*. **323**, 474 LP – 477 (2009).
- 688 64. Kato-Kataoka, A. *et al.* Soybean-derived phosphatidylserine improves memory function of
689 the elderly Japanese subjects with memory complaints. *J. Clin. Biochem. Nutr.* **47**, 246–
690 255 (2010).
- 691 65. Glade, M. J. & Smith, K. Phosphatidylserine and the human brain. *Nutrition* **31**, 781–786
692 (2015).
- 693 66. Zhou, M. *et al.* A central amygdala to zona incerta projection is required for acquisition
694 and remote recall of conditioned fear memory. *Nat. Neurosci.* **21**, 1515–1519 (2018).
- 695 67. Picelli, S. *et al.* Full-length RNA-seq from single cells using Smart-seq2. *Nat. Protoc.* **9**,
696 171–181 (2014).
- 697 68. Butler, A., Hoffman, P., Smibert, P., Papalexi, E. & Satija, R. Analysis Integrating single-
698 cell transcriptomic data across different conditions , technologies , and species. *Nat.*
699 *Biotechnol.* **36**, 411–420 (2018).
- 700

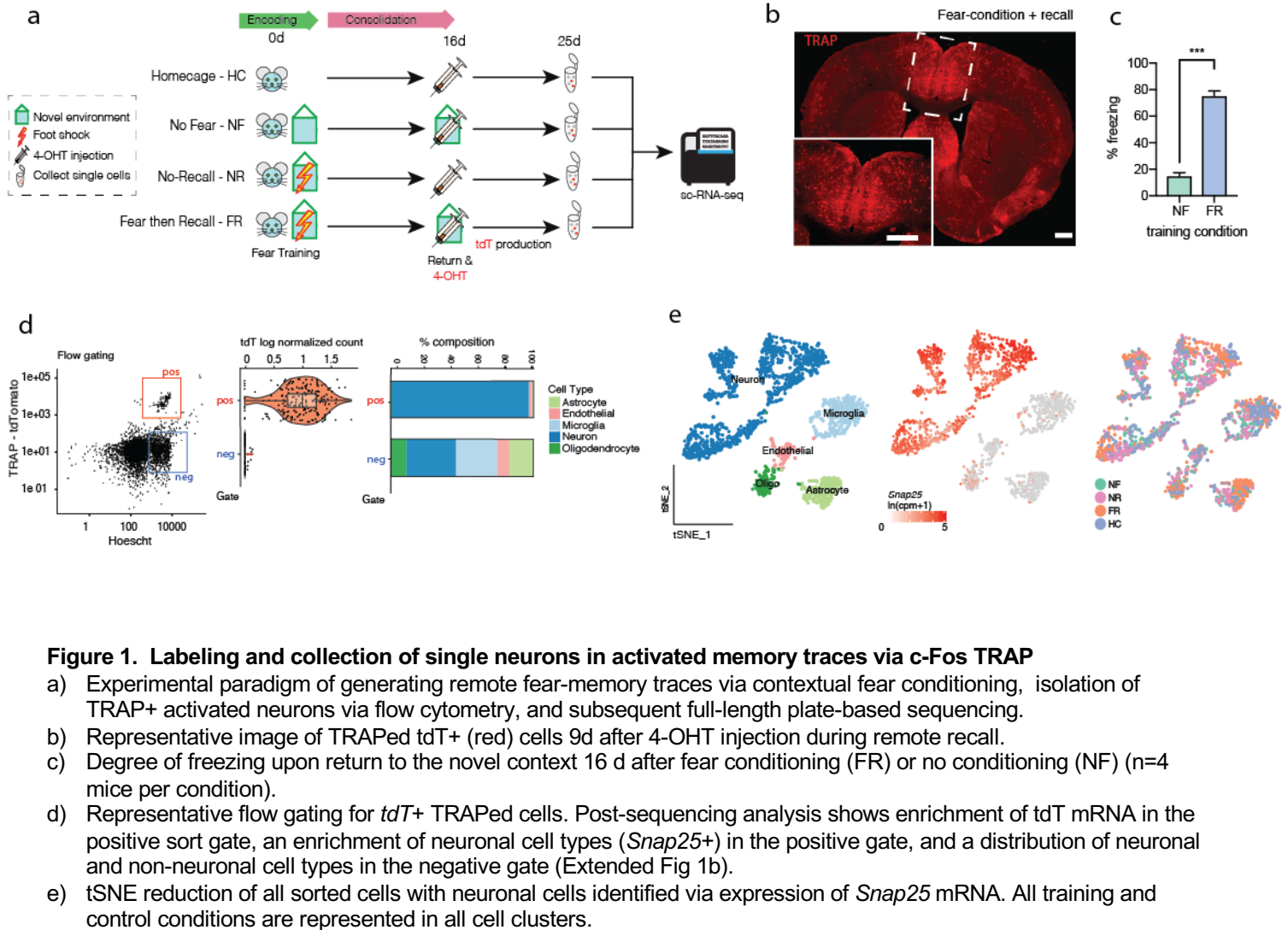


Figure 1. Labeling and collection of single neurons in activated memory traces via c-Fos TRAP

- Experimental paradigm of generating remote fear-memory traces via contextual fear conditioning, isolation of TRAP+ activated neurons via flow cytometry, and subsequent full-length plate-based sequencing.
- Representative image of TRAPed tdT+ (red) cells 9d after 4-OHT injection during remote recall.
- Degree of freezing upon return to the novel context 16 d after fear conditioning (FR) or no conditioning (NF) (n=4 mice per condition).
- Representative flow gating for tdT+ TRAPed cells. Post-sequencing analysis shows enrichment of tdT mRNA in the positive sort gate, an enrichment of neuronal cell types (*Snap25*⁺) in the positive gate, and a distribution of neuronal and non-neuronal cell types in the negative gate (Extended Fig 1b).
- tSNE reduction of all sorted cells with neuronal cells identified via expression of *Snap25* mRNA. All training and control conditions are represented in all cell clusters.

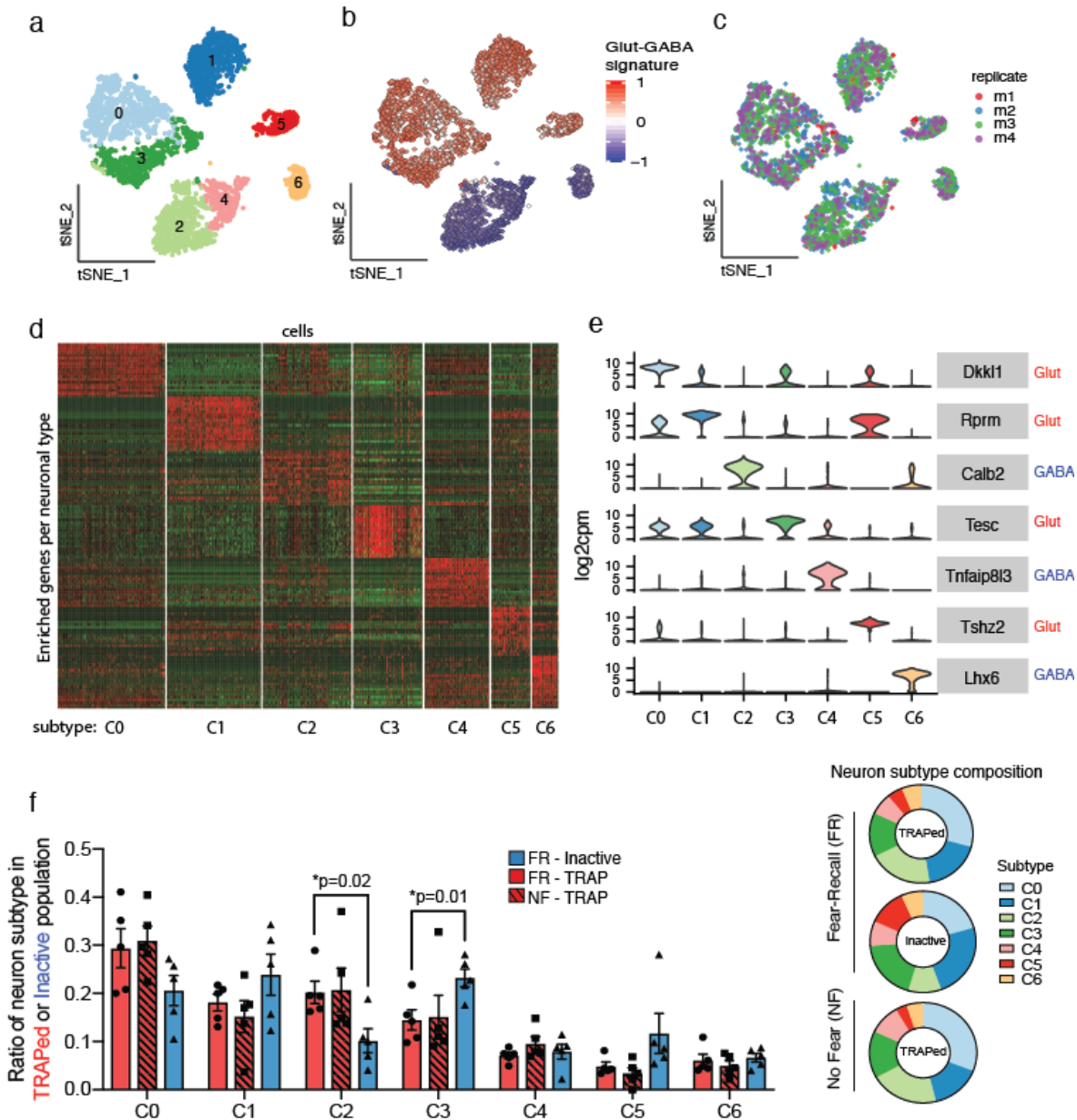
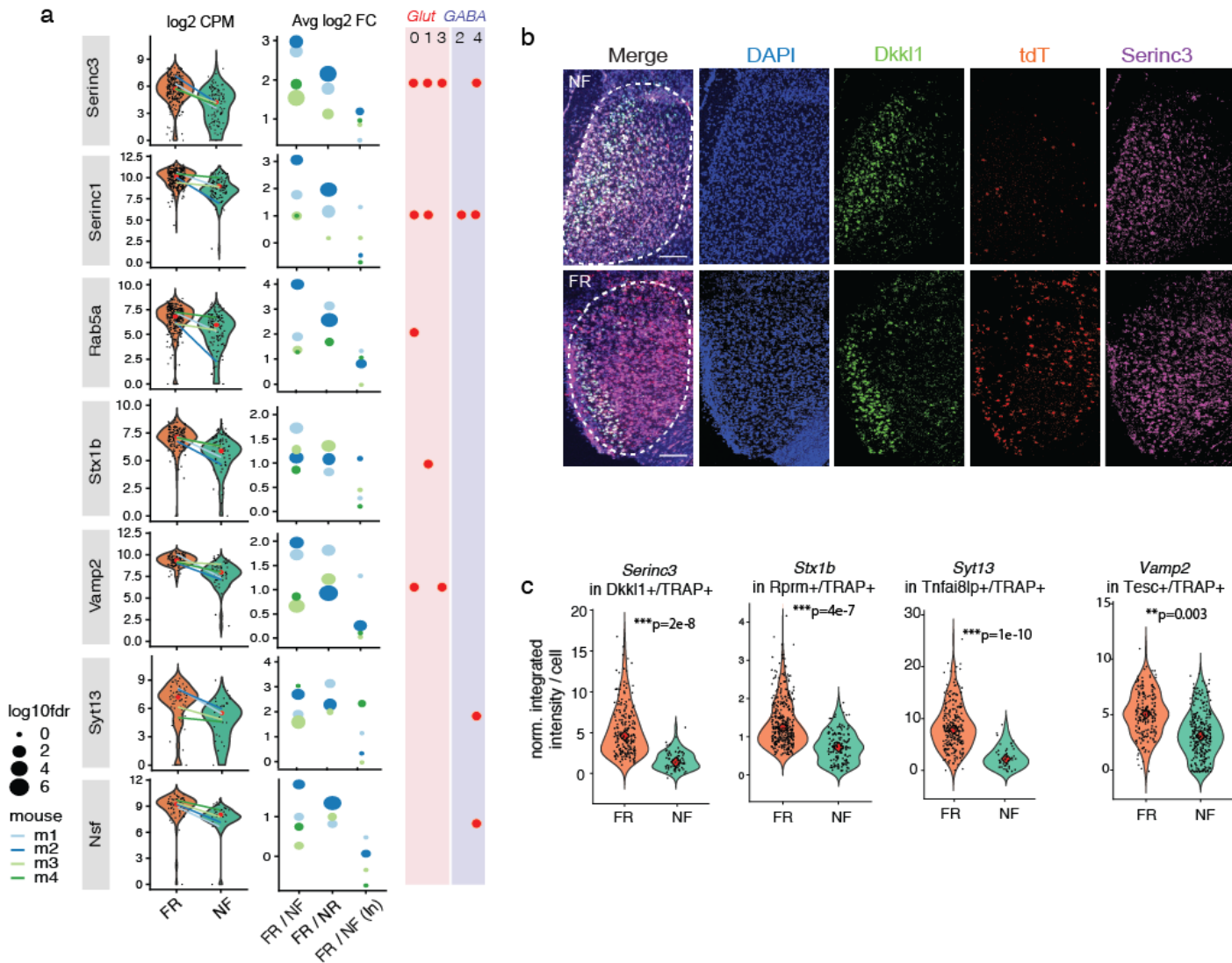


Figure 2. Molecular identification of activated neurons during consolidation in a remote memory trace.

- tSNE reduction and Louvain clustering of all *Snap25*+ neurons (total 3691 cells across 4 conditions) using the top 2500 variable features reveals 7 distinct neuronal subtype (C0-C6).
- Identification of excitatory (glutamatergic) and inhibitory (GABAergic). Glut-GABA signature is calculated based on the difference of the scaled expression level of *Gad1* and *Slc17a7*.
- Distribution of biological replicates between C0 to C6 subtypes for all training conditions combined.
- Heatmap depicting the top 25 enriched genes per neuron subtype and distinctiveness of their gene expression.
- Violin plots of expression of putative marker genes for each neuron subtype (C0 to C6) (from d).
- Bar plot of the differences in neuron subtype composition of TRAPed populations in FR and NF mice, as well as inactive populations in FR mice (n=5 mice/condition). Ring plots depict the distribution of neuronal types (C0-C6) in each group of cells collected.



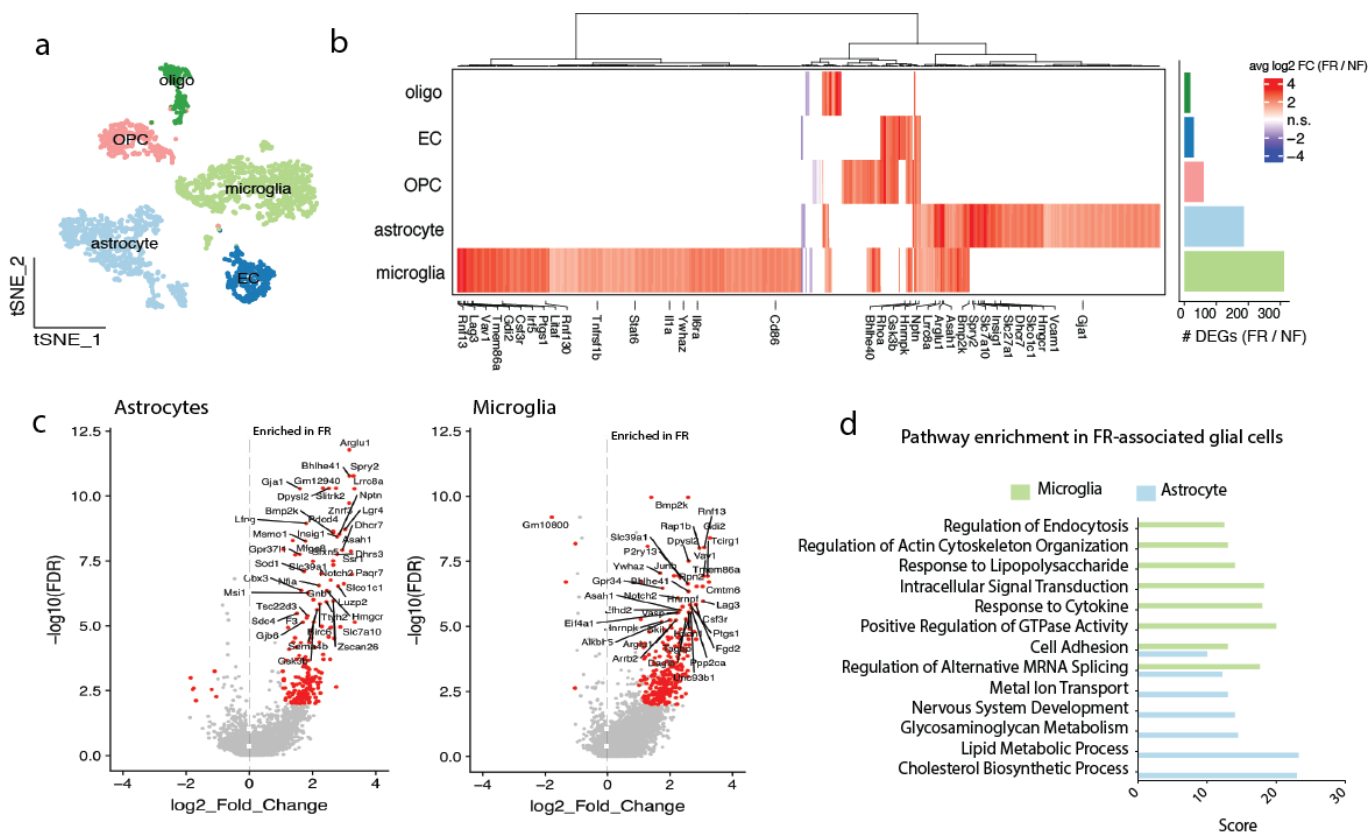


Figure 5. Non-neuronal cells exhibit significant transcriptional changes that are distinct from neurons

- (A) tSNE of all non-neuronal cells collected (collected in an unbiased manner from tdT- gates) reveal 5 cell types (astrocyte, endothelial, microglia, OPCs and oligodendrocytes).
- (B) Heatmap of DEGs in non-neuronal cells (FR over NF). DEGs are defined as $\log_2FC > 1$ and $FDR < 0.01$. Fold change of genes that do not pass this threshold are not displayed (white = not significant). Genes are clustered via the ward.D algorithm. Bar graph depicts the number of DEGs that satisfy this criteria in each non-neuronal cell type. Top DEGs for glial cells (astrocytes and microglia) that are also differentially expressed in FR vs NR, are labeled.
- (C) Volcano plots of DEGs up and downregulated in astrocytes and microglia in FR vs NF mice. DEGs ($FDR > 0.01$, $\log_2FC > 1$) are labeled in red, and exemplary DEGs (high \log_2FC and $-\log_{10}FDR$) are labeled in black.
- (D) GO biological function pathway analysis of the DEGs in microglia and astrocytes